

Exclusive vector meson production at HERA from QCD with saturation

C. M arquet

RIKEN BNL Research Center, Brookhaven National Laboratory, Upton, NY 11973, USA

R. Peschanski^yService de Physique Théorique, CEA/Saclay, 91191 Gif-sur-Yvette cedex, France
URA 2306, unité de recherche associée au CNRSG. Soyez^{zx}LPTHE, Université P. et M. Curie (Paris 6), Université D. Diderot (Paris 7)
Tour 24-25, 5e Etage, Bât. 126, 4 place Jussieu, 75252 Paris cedex 05, France
UMR 7589, unité mixte de recherche du CNRS

Following recent predictions that the geometric scaling properties of deep inelastic scattering data in inclusive p collisions are expected also in exclusive diffractive processes, we investigate the diffractive production of vector mesons. Using analytic results in the framework of the BK equation at non-zero momentum transfer, we extend the QCD-inspired saturation model to parametrize the momentum transfer dependence. We obtain a good fit to the available HERA data and make predictions for deeply virtual Compton scattering measurements.

I. INTRODUCTION

Geometric scaling [1] is a striking feature of deep inelastic scattering (DIS) data at small Bjorken x , or at large rapidity $Y = \log(1/x)$: The photon-proton total cross section $\sigma_{\text{tot}}^{\text{p} \times \text{p}}(x; Q^2)$ obeys a scaling in the single variable $Q^2 = Q_s^2(x)$ where Q is the virtuality of the photon and Q_s the saturation scale. This momentum scale increases with rapidity according to $Q_s^2(x) = Q_0^2 x$ with 0.3 and $Q_0 = 0.1$ GeV (giving a saturation scale of order 1 GeV for $x = 10^{-4}$). Recently, the diffractive cross-section $\sigma_{\text{di}}^{\text{p} \times \text{p}}$ and the elastic vector meson production cross-section $\sigma_{\text{VM}}^{\text{p} \times \text{p}}$ were shown to also feature scaling behaviours, with the same saturation scale [2].

From the theoretical point of view, the high-energy or small x limit can be studied within the QCD dipole picture [3]. Introducing the dipole-proton elastic scattering amplitude $T(r; Y)$, where r is the transverse size of the dipole, the corresponding law $T(r; Y) = T(r Q_s(Y))$ appears to be a genuine consequence of saturation effects [4] characteristic of the high-density regime of perturbative QCD. More precisely, the evolution towards saturation is conveniently described by the non-linear Balitsky-Kovchegov (BK) equation [5] that resums QCD fan diagrams in the leading-logarithmic approximation. Geometric scaling for $T(r; Y)$ appears to be a mathematical consequence of the asymptotic solution in Y of this nonlinear equation in terms of travelling waves [6]. Within this theoretical framework, $Q_s(Y) = Q_0 s(Y)$ and the rapidity dependence of the saturation scale, given by $s(Y)$, is then obtained from the features of the Balitsky-Fadin-Kuraev-Lipatov [7] (BFKL) kernel, which drives the linear regime of the BK evolution.

The total cross section $\sigma_{\text{tot}}^{\text{p} \times \text{p}}$ (as well as the diffractive cross section $\sigma_{\text{di}}^{\text{p} \times \text{p}}$ and the elastic vector meson production cross section $\sigma_{\text{VM}}^{\text{p} \times \text{p}}$) is related to the forward elastic dipole-proton amplitude. It is natural to ask the question whether geometric scaling survives when considering nonforward amplitudes. To that purpose, it is tempting to study the BK equation which is written for $T(r; b; x)$, the dipole-proton elastic scattering amplitude, depending not only on the dipole size r but also on the impact parameter b : However, the aforementioned scaling law cannot be easily adapted to account for the impact parameter dependence. The analysis of the BK equation in impact-parameter space [8, 9] even shows a contradiction with concern: the large- b dependence of the solutions develops a power-law tail with decreasing x :

Previous studies [10, 11] have shown that the travelling-wave method can be extended to the BK equation with transverse-space kinematical dependence provided one investigates the problem in terms of momentum transfer instead

^z on leave from the fundamental theoretical physics group of the University of Liège.

E electronic address: marquet@quark.phy.bnl.gov

^yE electronic address: pesch@spht.saclay.cea.fr^xE electronic address: g.soyez@ulg.ac.be

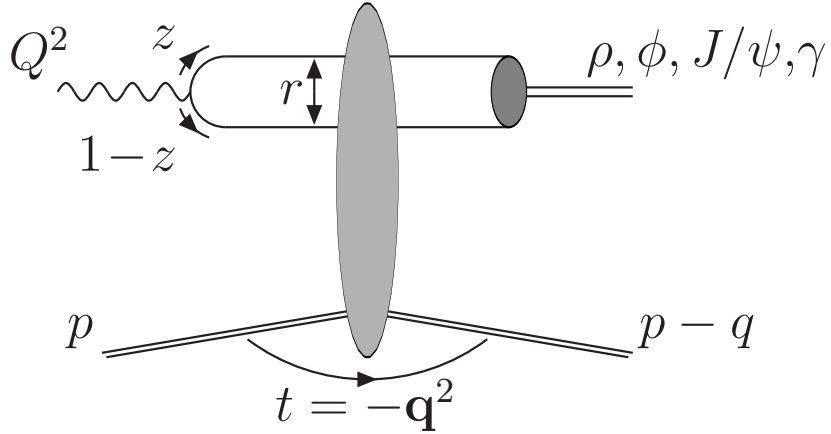


FIG. 1: Vector-particle production in the dipole frame. The amplitude factorises as a product of vertex functions and elastic dipole-proton interaction amplitude (see formul (2) and (4)).

of impact parameter. The remarkable point [10] is that the travelling-wave analysis of the BK equation can be better achieved in momentum space, by Fourier transforming $T(r; b; Y)$ into $T(r; q; Y)$ where q is the momentum transfer. From the knowledge of the exact solutions of the BFKL equation at non-zero momentum transfer [12], the travelling-wave property has been extended [10]:

at small momentum transfer, i.e. when $|r|q| < |r|b| \ll 1$; one has asymptotically $T(r; q; Y) = T(|r|b|_s(Y); q)$, recovering the forward result;

at intermediate, semi-hard, momentum transfer, i.e. when $|r|b| < |r|q| \ll 1$; one has asymptotically $T(r; q; Y) = T(|r|q|_s(Y); q)$:

This introduces a q -dependent saturation momentum with a rapidity evolution $_s(Y)$ keeping the same form as in the forward case. Those predictions were confirmed both by analytical and numerical analysis of the BK equation completely formulated in momentum space [11].

Our purpose here is to investigate an interesting phenomenological consequence of these results: the geometric scaling property should manifest itself in exclusive vector meson production and deeply virtual Compton scattering (DVCS) at nonzero momentum transfer $t = -q^2$. In this paper, we analyse whether or not the available data from HERA are sensitive to a t -dependent saturation scale. To do this, we use a QCD-inspired saturation model for the dipole amplitude $T(r; q; Y)$. It is also interesting to notice that this parametrisation, using the momentum transfer q instead of the impact parameter b , as suggested by this derivation of saturation effects in perturbative QCD, provides a fruitful phenomenological framework since the data are directly measured as a function of $t = -q^2$.

The plan of the paper is as follows. In section II, we recall the formulation of vector meson production and DVCS differential cross-sections in terms of the dipole scattering amplitude $T(r; q; x)$. In section III, we briefly explain the asymptotic travelling-wave properties of this amplitude and how they translate into geometric scaling at non-zero momentum transfer; we also introduce our QCD-inspired model for T . In Section IV, we present fits to the vector-meson production experimental data, discuss our results and present predictions for DVCS. Section V concludes.

II. EXCLUSIVE VECTOR MESON PRODUCTION IN DISATSMALL x

In the small x limit, it is convenient to describe the scattering of the photon in a particular frame, called the dipole frame, in which the virtual photon undergoes the hadronic interaction via a fluctuation into a colorless $q\bar{q}$ pair, called dipole, which then interacts with the target proton. The wavefunctions $_{f,h,h}^{\pm}(z; r; Q^2)$ describing the splitting of a virtual photon with polarization $\pm 0; \pm 1$ into a dipole are well known. The indices $h = \pm 1$ and $\bar{h} = \mp 1$ denote the helicities of the quark and the antiquark composing the dipole of flavor f . The wavefunctions depend on the virtuality Q^2 ; the fraction z of longitudinal momentum (with respect to the p collision axis) carried by the quark, and the two-dimensional vector r whose modulus is the transverse size of the dipole. Explicit formul for the QED functions $_{f,h,h}^{\pm}$ can be found in the literature [13] and are recalled in Appendix A.

The exclusive production of vector mesons is represented in Fig.1: the photon splits into a dipole of size r which scatters elastically, with transfer momentum q , off the proton and recombines into a vector meson whose mass we shall denote M_V : To describe this process, we need to introduce the wavefunctions $_{f,h,h}^{V;}(z;r;M_V^2)$ which describe the splitting of the vector meson with polarization i into the dipole. In fact, to compute the vector meson production amplitude pictured in Fig.1, we need the transverse (T) and longitudinal (L) overlap functions $_{T,L}^V = (_{+}^V + _{-}^V)/2$ and $_{L}^V = _0^V$ obtained through

$$_{f,h,h}^V(z;r;Q^2;M_V^2) = \int_0^Z dz \int_0^{Z_1} dy \int_0^r dx \, _{T,L}^V(z;x-y;Q^2;M_V^2) e^{iq \cdot y} T(x;y;Y) : \quad (1)$$

These functions depend on the meson wavefunctions $_{f,h,h}^{V;}$; and several different models exist in the literature [4, 15, 16]. We shall discuss two different choices later in this paper: the light-cone Gaussian (LCG) wavefunctions [16] and the boosted Gaussian (BG) wavefunctions [14]. For completeness, we give explicit expressions for those overlap functions in Appendix A.

If q denotes the transverse momentum transferred by the proton during the collision, the differential cross-section with respect to $t = q^2$ reads

$$\frac{d_{T,L}^{p! V p}}{dt} = \frac{1}{16} \int_0^Z dz \int_0^{Z_1} dy \int_0^r dx \, _{T,L}^V(z;x-y;Q^2;M_V^2) e^{iq \cdot y} T(x;y;Y) : \quad (2)$$

where x and y are respectively the transverse positions of the quark and the antiquark forming the dipole. $T(x;y;Y)$ is the dipole-proton scattering amplitude and carries all the energy dependence via the rapidity Y which is now obtained from the centre-of-mass energy W and the vector meson mass M_V using

$$Y = \log \frac{W^2 + Q^2}{M_V^2 + Q^2} : \quad (3)$$

It is convenient to consider the dipole-proton scattering amplitude as a function of $r = x - y$ and $b = zx + (1 - z)y$ and to introduce the following Fourier transform :

$$T(r;q;Y) = \int_0^Z dz b e^{iq \cdot b} T(r;b;Y) : \quad (4)$$

Indeed, as we shall discuss in the next section, this quantity features the geometric scaling property at non-zero momentum transfer. The formula we shall use finally reads

$$\frac{d_{T,L}^{p! V p}}{dt} = \frac{1}{16} \int_0^Z dz \int_0^{Z_1} dy \int_0^r dx \, _{T,L}^V(z;r;Q^2;M_V^2) e^{izq \cdot r} T(r;q;Y) : \quad (5)$$

Note that formula (4) can also be used to compute the DVCS cross-section $^{p!} p$; provided one uses the vertex for a real photon instead of a vector meson in (1). The overlap function between the incoming virtual photon and the outgoing transversely-polarized real photon is now model-independent and given by

$$_{T,L}(z;r;Q^2) = \int_0^Z dz \int_0^{Z_1} dy \int_0^r dx \, _{f,h,h}^{T;}(z;r;0) \, _{f,h,h}^{T;}(z;r;Q^2) : \quad (6)$$

III. GEOMETRIC SCALING AT NON-ZERO MOMENTUM TRANSFER

We have expressed the exclusive vector meson production cross-sections (4) in the high-energy limit in terms of the Fourier-transformed dipole scattering amplitude off the proton $T(r;q;Y)$: Its evolution towards large values of Y is computable from perturbative QCD and the most important result about the growth of the dipole amplitude towards the saturation regime is probably the geometric scaling regime. It first appeared in the context of the proton structure function, which involves the dipole scattering amplitude at zero momentum transfer. At small values of x , instead of being a function of a priori the two variables $r = |r|$ and Y , the dipole scattering amplitude is actually a function of the single variable $r^2 Q_s^2(Y)$ up to inverse dipole sizes significantly larger than the saturation scale $Q_s(Y)$: More precisely, one can write

$$T(r;q=0;Y) = 2 R_p^2 N(r^2 Q_s^2(Y)) ; \quad (6)$$

implying (for massless quarks) the geometric scaling of the total cross-section at small x : $\frac{p!}{\text{tot}} x (Y; Q^2) = \frac{p!}{\text{tot}} x (Q^2 = Q_s^2(Y))$: This has been confirmed by experimental data [1] (see also [2] for the geometric scaling of the diffractive and elastic vector-meson production cross-sections) with $Q_s^2(Y) = Q_0^2 e^Y$; and the parameters 0.3 and $Q_0 = 0.1$ GeV.

As explained in the Introduction, it has been shown in a recent work [10, 11] that the geometric scaling property can be extended to the case of non zero momentum transfer, provided $r \gg 1$. We obtained that equation (6) can be generalised to

$$T(r; q; Y) = 2 R_p^2 f(q) N(r^2 Q_s^2(Y; q)); \quad (7)$$

with the asymptotic behaviours $Q_s^2(Y; q) = \max(Q_0^2; q^2) \exp(Y)$ and an unknown form factor $f(q)$ of non-perturbative origin.

In practice, we need to specify three ingredients:

The q dependence of the saturation momentum is parametrised as

$$Q_s^2(Y; q) = Q_0^2 (1 + \alpha q^2) e^Y \quad (8)$$

in order to interpolate smoothly between the small and intermediate transfer regions.

The form factor $f(q)$ catches the transfer dependence of the proton vertex. It has to be noticed that this form factor is factorised from the projectile vertices and thus does not spoil the geometric scaling properties. For simplicity, we use $f(q) = \exp(-B q^2)$.

The scaling function N is obtained from the forward saturation model [7]:

$$N(r Q_s(Y); Y) = \begin{cases} N_0 \frac{r^2 Q_s^2(Y)}{4}^c \exp^h \frac{\ln^2(r^2 Q_s^2(Y) - 4)}{2Y}^i & \text{for } r^2 Q_s^2(Y) \leq 4 \\ \frac{1}{e^{\ln^2(r^2 Q_s^2(Y))}} & \text{for } r^2 Q_s^2(Y) > 4 \end{cases} \quad (9)$$

with c and h are uniquely determined from the conditions that N and its derivative are continuous at $r^2 Q_s^2(x) = 4$: The coefficients $c = 0.6275$ and $h = 9.9$ are determined from the BFKL kernel. The amplitude at the matching point is taken as $N_0 = 0.7$ and the remaining parameters are fitted to the HERA measurements of the proton structure function: $c = 0.253$; $Q_0 = 0.206$ GeV, and $R_p = 3.25$ GeV¹. Note that the last factor in the expression for small dipole sizes introduces geometric scaling violations as predicted by QCD. It controls the way how geometric scaling is approached. Indeed, it can be neglected for $\log(r^2 Q_s^2 - 4) < 2Y$, meaning that the geometric scaling window extends like Y above the saturation scale (in logarithmic units).

The final expression of our QCD-based saturation model is thus

$$T(r; q; x) = 2 R_p^2 e^{B q^2} N(r Q_s(x; q); Y) \quad (10)$$

which is an extension of the forward model [7] including the QCD predictions for non zero momentum transfer. Indeed, this model reproduces the initial model for $q = 0$ and ensures that the saturation scale has the correct asymptotic behaviours. We have two parameters: c related to the scale at which the q dependence of the saturation scale becomes important and B ; the total slope of the form factor that we have taken as simple as possible. Those parameters have to be fitted to the experimental measurements of elastic vector-meson production as we shall comment in details in the next section. Before, note that the form factor depends on a single slope B ; independently of the vector-meson in the final state.

Indeed, this model reproduces the initial model for $q = 0$ and ensures that the saturation scale has the correct asymptotic behaviours. We have two parameters: c related to the scale at which the q dependence of the saturation scale becomes important and B ; the total slope of the form factor that we have taken as simple as possible. Those parameters have to be fitted to the experimental measurements of elastic vector-meson production as we shall comment in details in the next section. Note that the form factor depends on a single slope B ; independently of the vector-meson in the final state.

IV. FIT RESULTS AND DISCUSSION

In this section, we compare our formulation (4) and (10) for vector-meson production with the experimental measurements of and elastic production. We shall first state explicitly the data used to perform the fit, then give more details concerning the fit itself, present our results and compare them with other possible approaches, and finally we shall give predictions for D VCS measurements.

VM	Quantity	N _{pts}	t-dependent Q _s		t-independent Q _s	
			2	$^2 = N_{pts}$	LCG	B = cst.
	e1	47	54.297	1.156	1.688	1.732
	$\frac{d}{dt}$	50	69.097	1.382	1.620	1.489
	e1	34	44.932	1.322	0.830	2.247
	$\frac{d}{dt}$	70	76.307	1.076	0.945	0.931
Total		201	243.632	1.212	1.267	1.480
						1.245

TABLE I: χ^2 results of the fits to the vector-meson production data. The default values (with BG meson wavefunctions) are compared with values obtained when using alternative meson wavefunctions or models, for which the χ^2 per point is given.

Parameter	t-dependent Q _s			t-independent Q _s	
	our model (BG)	our model (LCG)		B = cst.	B = B ($Q^2 + M_V^2$)
c (GeV ²)	3.776	0.540	5.172	0.585	—
B (GeV ²)	3.740	0.141	3.894	0.130	2.412 0.043
B ⁰	—	—	—	—	1.674 0.107
					3.827 0.552

TABLE II: Parameters obtained from the fits.

A. Data selection

In this analysis, we shall include the differential cross-section d/dt as well as the elastic cross-section e_1 . The dataset is obtained from the π^+ meson production measured by H1 [18] and the π^- meson production measured by ZEUS [19]. We have not taken into account the ZEUS data for π^0 mesons [20] since they lie in the low- Q^2 region where we do not expect the condition $r_{\pi\pi} \gg Q^2$ to be valid. Also, we keep the same parameters as in [17] for $t=0$ as they provide a good description of the inclusive F_2 data. Since those results were obtained with light quarks only ($m_{u,d,s} = 140$ MeV, no charm), we postpone the extension of our model to J/ψ production to a future work. The ratio $R = \frac{\sigma_L}{\sigma_T}$ between the longitudinal and transverse elastic cross-sections is mostly dependent of the choice of wavefunction, hence we have not included it in the analysis. Finally, this gives a total of 201 data points which have to be reproduced with the two parameters B and c in equation (10).

B. Meson wavefunctions and alternative models

We shall test the dependence of our results with respect to the choice of the model used for vector-meson wavefunctions. While we shall by default use the Boosted Gaussian (BG) which has already proven to give good results for vector-meson production, we shall also study the LCG case in order to understand to what extend our results depend upon the model for wavefunctions.

In order to test the quality of our parametrisation with the dependent saturation scale, we shall compare our results with two alternative parametrisations. Since the main aim of this work is to analyse the t-dependence of the saturation scale, the first alternative we shall consider is a model in which we only adjust the slope B while keeping the saturation scale independent of the momentum transfer. For the second alternative, we notice that if one assumes a slope B for the differential cross-sections at a given W and Q^2 , the slope is experimentally observed to depend on Q^2 : Within our parametrisation, it is the t-dependence of the saturation scale which is expected to account for this behaviour in Q^2 : This will be compared with a model where we keep Q_s constant in t ($c = 0$) and explicitly introduce a Q^2 dependence of the slope B . We shall use $B(Q^2) = B + B^0(Q^2 + M_V^2)$; which shows the same trend as the experimental estimations of $B(Q^2)$: Note however that this last two-parameter model is not compatible with the factorisation formula (4), valid at small values of x ; where only the wavefunctions depend explicitly on Q^2 .

C. Results

We show in Table I the χ^2 corresponding to the fits of the different models presented above to the specified data. The parameters associated with those fits are given in Table II. In both tables, successive columns show the results

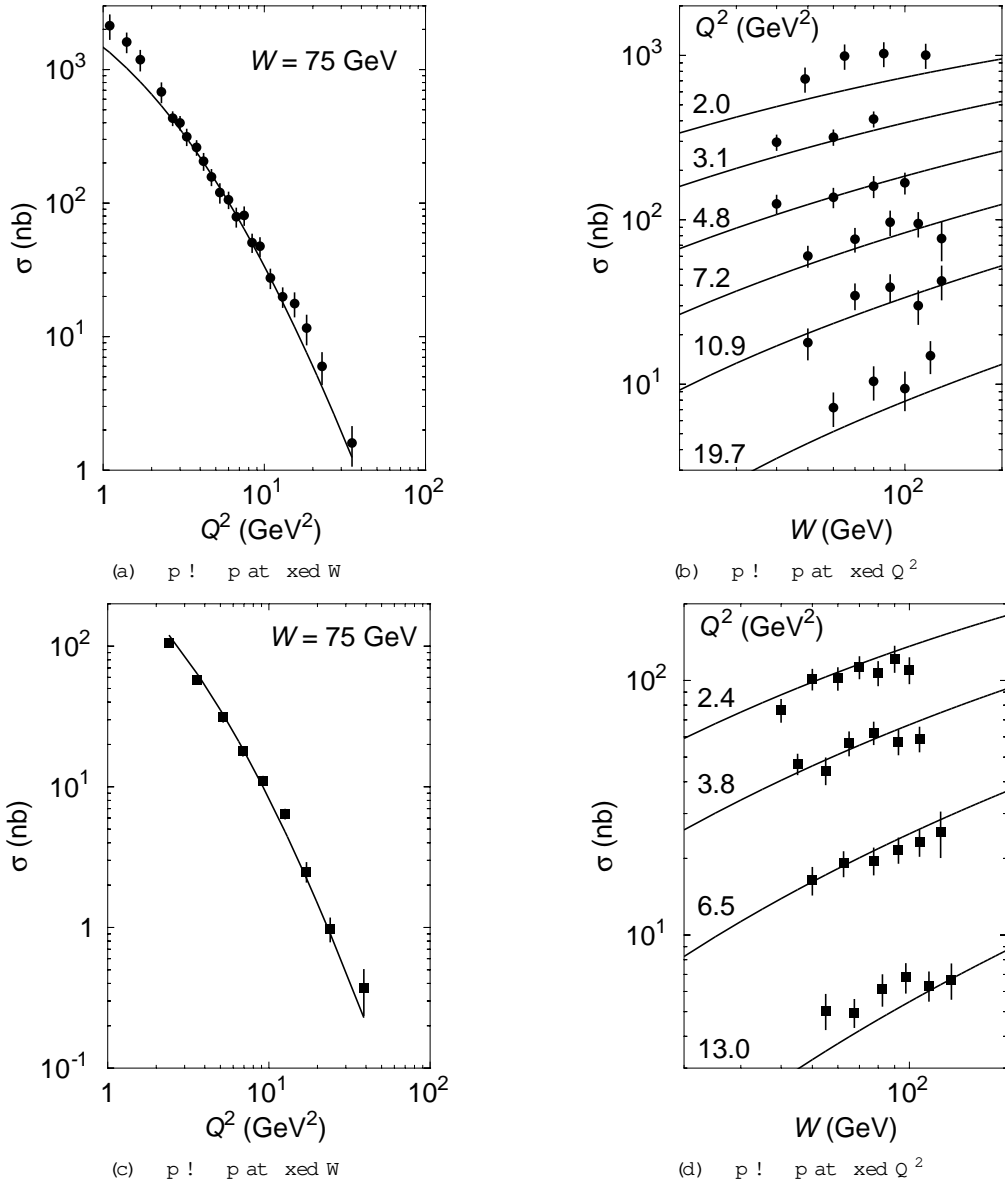


FIG. 2: Fit results for the (H1 [18]) and (ZEUS [19]) elastic cross-sections.

for our model with t -dependent saturation scale convoluted with BG wavefunctions (we give both the Q^2 and the W per data point for that model, while only the latter is given for other models), followed by the same model with LCG wavefunctions, and then the two alternative models without momentum-transfer-dependence in the saturation scale (using BG wavefunction).

Those results show that our approach gives good results for vector meson production and this is confirmed by Figures 2 and 3 on which we have plotted the curves for our t together with the experimental data points. For comparison with the other parametrizations, we have displayed in Figure 4 the curves corresponding to the three parametrizations of Table I (our t -dependent parametrization for the BG wavefunctions together with the two t -independent ones) for π^+ - and π^- meson differential cross-sections for the lower and higher available values of Q^2 .

Some comments are in order:

We obtained good fits with both the BG and LCG wavefunctions. The LCG results, which are quite sensitive to the kind of vector meson produced, are better for the π^+ meson while the BG results are better in the π^- meson case. Globally, the BG Q^2 is slightly better than LCG one.

Comparing fits performed with our parametrization 10) and the corresponding one with a t -independent

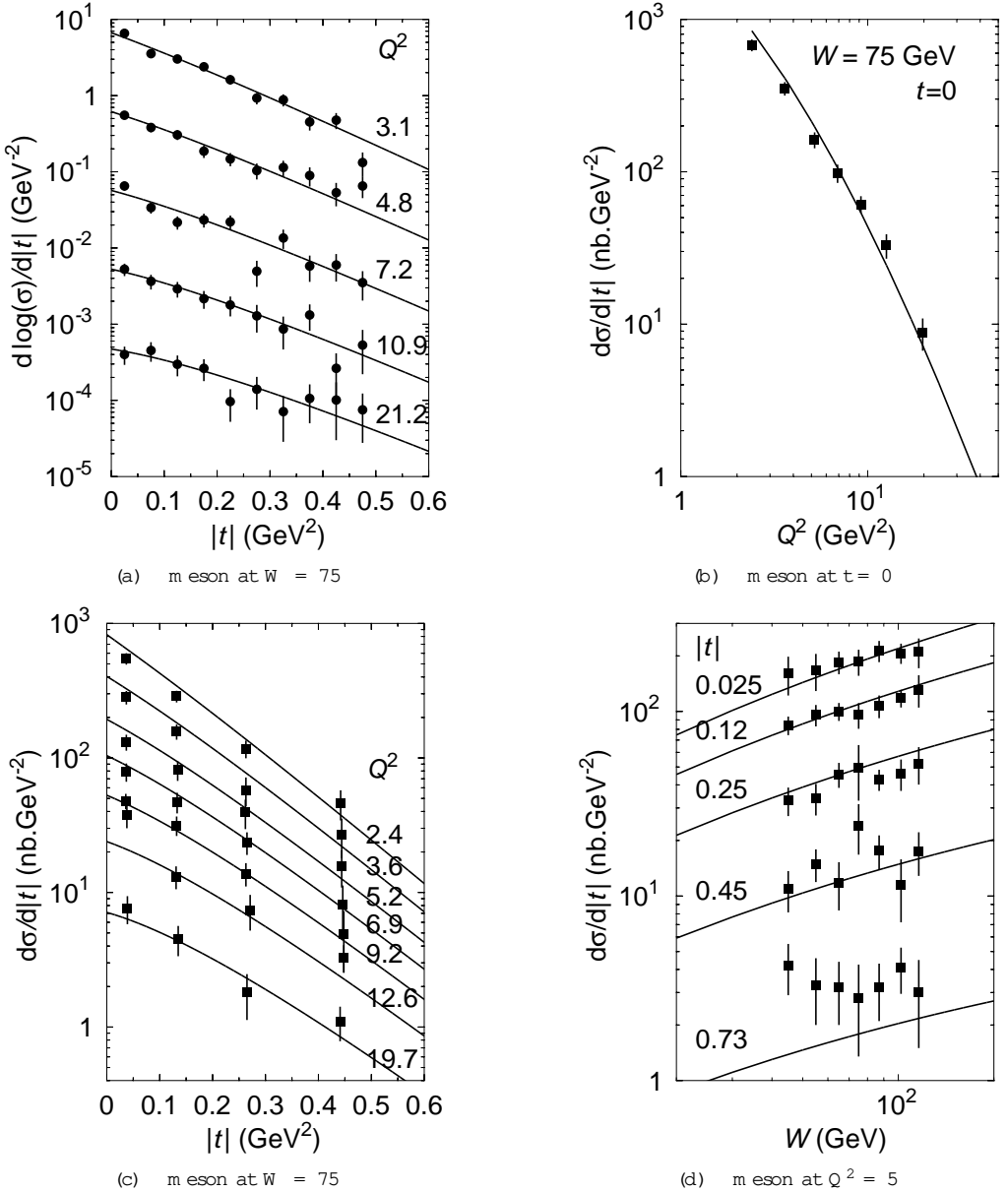


FIG. 3: Fit results for the (H1 [18]) and (ZEUS [19]) differential cross-section.

saturation scale and constant slope, one sees that the introduction of $Q_s(t)$ significantly improves the fit. This significant result, which is consistent with theoretical expectations, opens the way for further experimental test of the saturation regime of QCD with exclusive processes.

Compared to our parametrisation, the parametrisation with a t independent saturation scale and with $B(\hat{Q}) = B + B^0 = (Q^2 + M_V^2)$ shows Q^2 values lower in the π -meson case but higher in the η -meson case. The global Q^2 is slightly higher than that of our QCD-inspired model, in which this effective behaviour in Q^2 is accounted for by the dependence of the saturation scale.

From the value of the parameter $c = 3.78 \text{ GeV}^2$ obtained in our approach, we can say that the saturation scale starts to increase with momentum transfer when $t \approx c^{-1} = 0.265 \text{ GeV}^2$. It is interesting that this scale lies within the range of accessible data meaning that we can get insight on the dynamics of saturation by looking at the present HERA data.

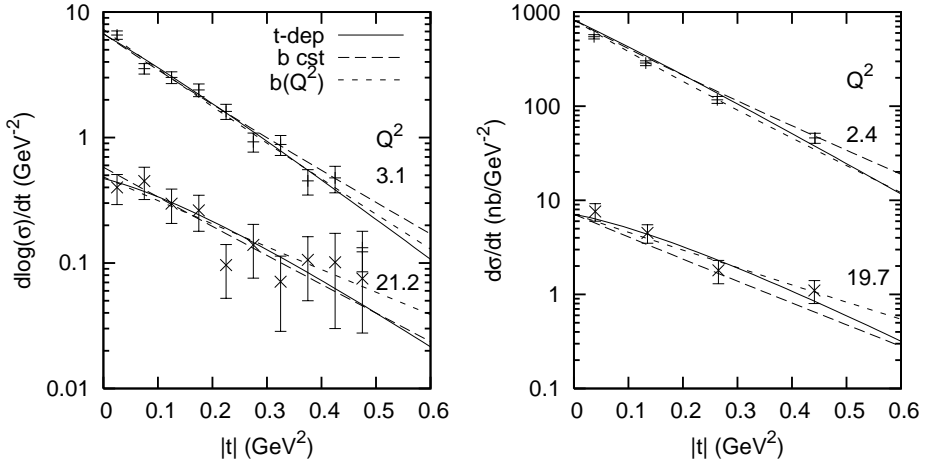


FIG. 4: Comparison of the three parametrizations for differential cross-sections. The left plot shows the ρ meson production at $Q^2 = 3.1$ and 21.2 GeV and the right plot corresponds to the ρ meson at $Q^2 = 2.4$ and 19.7 GeV. Continuous lines: t -dependent saturation; Fat-dashed lines: t -independent saturation, fixed slope; Thin-dashed lines: Q^2 -dependent slope.

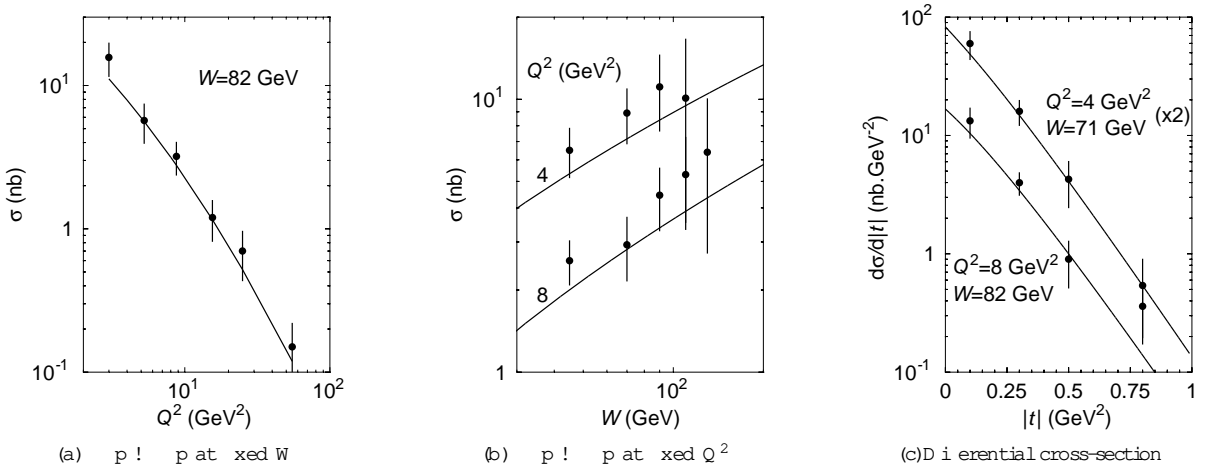


FIG. 5: Predictions for the DVCS measurements. The data are from H1 [21].

D. Predictions for DVCS

Using the overlap function (5) in formula (4), we obtain the DVCS cross-section. The predictions obtained with our model and the parameters determined above are presented in Figure 5. They are compared with a few available data [21] and the agreement is good. Because of the error bars are quite large, these data do not alter the fit described previously, when included. Our predictions will be further tested with forthcoming DVCS data.

V. CONCLUSIONS AND PERSPECTIVES

Following the theoretical observation that geometric scaling property of the BK saturation equation is valid not only for inclusive but also for differential exclusive processes of DIS, we have proposed an extension of the parametrization [17] (see formula (10)) to non-forward vector-meson production. The theoretical analysis predicts a saturation scale proportional to t and a factorisation of the nonperturbative proton form factor. Hence, the geometric scaling property, i.e. the $Q = Q_s(Y)$ scaling, is preserved at non-zero momentum transfer with $Q_s(t; Y) = f_s(Y) f(t)$, and $f(t)$ interpolating between the soft scale at small t and $f(t)$ at higher t .

By introducing two parameters to feature the predicted behaviour of the saturation scale with t (see (8)) and the factorised nonperturbative proton form factor (see (10)), we satisfactorily describe the available HERA data for

exclusive di ractive - and -meson production.

This good agreement with the data, shows the consistency between QCD saturation predictions and measurements in the HERA energy range. We shall be able to further test our parametrization when the preliminary ; ; and DVCS data become final. We also leave for future work the inclusion of $J=$ production, which implies to first reanalyse the F_2 data including the charm quark to obtain the saturation scale parameters for the forward model.

Other successful models of exclusive processes with saturation effects have already been achieved [22, 23, 24] confirming the interest of saturation physics for vector-meson production. However we would like to emphasize the specific aspect of the present work, which may open a new way to describe exclusive measurements in DIS. Indeed, within our approach we use the momentum transfer q instead of the impact parameter b ; to parametrize the saturation scale. Instead, this q -dependence is expected from p-QCD while the nonperturbative dependence in q is factorised, which is not the case in impact-parameter space. This is also practically convenient since the data are directly measured as a function of $t = -q^2$:

Acknowledgments

We would like to thank Barbara Clerbaux, Laurent Favart, Alessia Brunni, Allen Caldwell and Miro Heibich for helping us collecting the HERA vector-meson production data. We also thank Laurent Schael and Christophe Royon for insightful discussions concerning DVCS and Jean-Rene Cudell for useful clarifications concerning the alternative models. C.M. is supported in part by RIKEN, Brookhaven National Laboratory and the U.S. Department of Energy DE-AC02-98CH10886]. C.M. and G.S. also thank the Galileo Galilei Institute for Theoretical Physics for hospitality and the INFN for partial support when this work was completed. G.S. is funded by the National Funds for Scientific Research (Belgium). G.S. also wants to thank the SPhT (Saclay) for hospitality when this work was started.

APPENDIX A : PHOTON AND VECTOR-MESON WAVEFUNCTIONS

For the self-consistency of the paper, let us give the expressions for the overlap functions we have used in (4) for the different processes. According to equation (4), they are the product of a wavefunction for the splitting $q \rightarrow q \bar{q}$ and a factor accounting for the production of the final state $q \bar{q} \rightarrow ; ; V$, appropriately summed over the helicity and flavor indices.

When the final state is a photon (real or virtual), all vertices can be computed from perturbative QED at lowest order in the electromagnetic coupling. The results are

$$\begin{aligned} {}_L^X(z; r; Q^2) &= \sum_f \frac{e_f^2}{2} \frac{eN_c}{2} 4Q^2 z^2 (1 - z)^2 K_0^2(rQ_f); \\ {}_T^X(z; r; Q^2) &= \sum_f \frac{e_f^2}{2} \frac{eN_c}{2} [z^2 + (1 - z)^2] Q_f^2 K_1^2(rQ_f) + m_f^2 K_0^2(rQ_f); \\ {}_T^X(z; r; Q^2) &= \sum_f \frac{e_f^2}{2} \frac{eN_c}{2} [z^2 + (1 - z)^2] Q_f K_1(rQ_f) m_f K_1(rm_f) + m_f^2 K_0(rQ_f) K_0(rm_f); \end{aligned}$$

where e_f and m_f denote the charge and mass of the quark with flavor f and with $Q_f^2 = z(1 - z)Q^2 + m_f^2$: In practice, we sum over three flavors.

When the final state is a vector meson, the light-cone wavefunctions are usually parametrized in terms of an additional unknown vertex function for which there exists different models. The expressions to be used in (4) are then (for a vector-meson V)

$$\begin{aligned} {}_L^V(z; r; Q^2) &= \hat{e}_f \frac{r}{4} \frac{eN_c}{2} 2Q K_0(rQ_f) M_V z (1 - z) {}_L^V(r; z) + \frac{m_f^2}{M_V} \frac{r^2}{r} {}_L^V(r; z); \\ {}_T^V(z; r; Q^2) &= \hat{e}_f \frac{r}{4} \frac{eN_c}{2} \frac{eN_c}{2} m_f^2 K_0(rQ_f) {}_T^V(r; z) [z^2 + (1 - z)^2] Q_f K_1(rQ_f) @_r {}_T^V(r; z); \end{aligned}$$

where the constant \hat{e}_f stands for an effective charge. It is given in table III along with the quark and meson masses used. Those expressions are very similar to the ones used for photons except for the function ${}_L, {}_T^V$ that is related to

the vertex function and depends on the model. In the present work, we have used the boosted Gaussian model which is a simplified version of the Nemchik, Nikolaev, Predazzi and Zakharov model [4]:

$$N_{L,T} = N_{L,T} \exp \left[-\frac{m_f^2 R^2}{8z(1-z)} + \frac{m_f^2 R^2}{2} - \frac{2z(1-z)r^2}{R^2} \right]^{\frac{1}{2}}$$

The parameters R and $N_{L,T}$ are constrained by unitarity of the wavefunction as well as by the electronic decay widths. They are given in table III.

Vector meson	M_V (GeV)	m_f (GeV)	ϵ_f	R^2 (GeV 2)	N_L	N_T
	0.776	0.14	$1/\sqrt{2}$	12.9	0.853	0.911
	1.019	0.14	1/3	11.2	0.825	0.919

TABLE III: Parameters for the vector meson light-cone wavefunctions.

[1] A.M. Stasto, K. Golec-Biernat and J. Kwiecinski, Phys. Rev. Lett. 86 (2001) 596. For a recent discussion, see F. Gelis, R. Peschanski, G. Soyez and L. Schœuel, "Systematics of geometric scaling," arXiv:hep-ph/0610435.

[2] C. Marquet and L. Schœuel, Phys. Lett. B 639 (2006) 471.

[3] A.H. Mueller, Nucl. Phys. B 335 (1990) 115;
N.N. Nikolaev and B.G. Zakharov, Zeit. für. Phys. C 49 (1991) 607.

[4] E. Iancu, K. Itakura and L.M. Clerman, Nucl. Phys. A 724, 181 (2003) [arXiv:hep-ph/0212123].

[5] I. Balitsky, Nucl. Phys. B 463 (1996) 99; Phys. Lett. B 518 (2001) 235;
Yu.V. Kovchegov, Phys. Rev. D 60 (1999) 034008; Phys. Rev. D 61 (2000) 074018.

[6] S. Munier and R. Peschanski, Phys. Rev. Lett. 91 (2003) 232001; Phys. Rev. D 69 (2004) 034008; D 70 (2004) 077503.

[7] L.N. Lipatov, Sov. J. Nucl. Phys. 23 (1976) 338;
E.A. Kuraev, L.N. Lipatov and V.S. Fadin, Sov. Phys. JETP 45 (1977) 199;
I.I. Balitsky and L.N. Lipatov, Sov. J. Nucl. Phys. 28 (1978) 822.

[8] A. Kovner and U.A.W. Hebecker, Phys. Rev. D 66 (2002) 051502; Phys. Lett. B 551 (2003) 311;
E. Ferreiro, E. Iancu, K. Itakura and L.M. Clerman, Nucl. Phys. A 710 (2002) 373.

[9] K. Golec-Biernat and A.M. Stasto, Nucl. Phys. B 668 (2003) 345;
E. Oktesson, M. Kozlov, E. Levin, U. Maor and E. Neftekhali, Nucl. Phys. A 742 (2004) 55.

[10] C. Marquet, R. Peschanski and G. Soyez, Nucl. Phys. A 756 (2005) 399.

[11] C. Marquet and G. Soyez, Nucl. Phys. A 760 (2005) 208.

[12] L.N. Lipatov, Sov. Phys. JETP 63 (1986) 904;
H. Navelet and R. Peschanski, Nucl. Phys. B 507 (1997) 353.

[13] J.D. Bjorken, J.B. Kogut and D.E. Soper, Phys. Rev. D 3 (1971) 1382.

[14] J. Nemchik, N.N. Nikolaev and B.G. Zakharov, Phys. Lett. B 341 (1994) 228 [arXiv:hep-ph/9405355]; J. Nemchik, N.N. Nikolaev, E. Predazzi and B.G. Zakharov, Z. Phys. C 75 (1997) 71 [arXiv:hep-ph/9605231].

[15] L. Frankfurt, W. Koepf and M. Strikman, Phys. Rev. D 54 (1996) 3194.

[16] H.G. Dosch, T. Gousset, G. Kulzinger and H.J. Pirner, Phys. Rev. D 55 (1997) 2602;
G. Kulzinger, H.G. Dosch and H.J. Pirner, Eur. Phys. J. C 7 (1999) 73.

[17] E. Iancu, K. Itakura and S. Munier, Phys. Lett. B 590 (2004) 199.

[18] C. Adloff et al. [H1 Collaboration], Eur. Phys. J. C 13 (2000) 371 [arXiv:hep-ex/9902019].

[19] S. Chekanov et al. [ZEUS Collaboration], Nucl. Phys. B 718 (2005) 3 [arXiv:hep-ex/0504010].

[20] J. Breitweg et al. [ZEUS Collaboration], Eur. Phys. J. C 6 (1999) 603 [arXiv:hep-ex/9808020].

[21] A. Aktas et al. [H1 Collaboration], Eur. Phys. J. C 44 (2005) 1 [arXiv:hep-ex/0505061].

[22] S. Munier, A.M. Stasto and A.H. Mueller, Nucl. Phys. B 603 (2001) 427.

[23] H. Kowalski and D. Teaney, Phys. Rev. D 68 (2003) 114005;
H. Kowalski, L. Motyka and G. Watt, Phys. Rev. D 74 (2006) 074016.

[24] J.R. Forshaw, R. Sandapen and G. Shaw, JHEP 0611 (2006) 025 [arXiv:hep-ph/0608161]; Phys. Rev. D 69 (2004) 094013 [arXiv:hep-ph/0312172].